RADIOFREQUENCY GASEOUS DETECTION DEVICE (RF-GDD)

Gerasimos D. Danilatos

ESEM Research Laboratory, 98 Brighton Boulevard, North Bondi, NSW 2026, AUSTRALIA

Telephone +61 2 91302837

Fax +61 2 93650326

Email esem@bigpond.com

Running title: RADIOFREQUENCY GASEOUS DETECTION DEVICE

Key words: radiofrequency, ESEM, SEM, detection, environmental, amplifier, discharge.

Abstract

A radiofrequency gaseous detection device is proposed for use with instruments employing charged particle beams, such as electron microscopes and ion beam technologies, as well as for detection of ionising radiations as in proportional counters. An alternating (oscillating) electromagnetic field in the radiofrequency range is applied in a gaseous environment of the instrument. Both the frequency and amplitude of oscillation are adjustable. The electron or ion beam interacts with a specimen and releases free electrons in the gas. Similarly, an ionising radiation source releases free electrons in the gas. The free electrons are acted upon by the alternating electromagnetic field and undergo an oscillatory motion resulting in multiple collisions with the gas molecules, or atoms. At sufficiently low pressures, the oscillating electrons also collide with surrounding walls. These processes result in an amplified electron signal and an amplified photon signal in a controlled discharge. The amplified signals, which are proportional to the initial number of free electrons, are collected by suitable means for further processing and analysis.

Introduction

The gaseous detection device (GDD) has become the standard means for detection and imaging in the environmental scanning electron microscope (ESEM). The theory and practice of this device has been extensively reported by Danilatos (1986; 1988; 1990a; 1990b; 1990c; 1992, 1993). It is based on the use of the environmental gas of an ESEM to detect and amplify various ionising signals via a controlled electron avalanche in a manner similar to that used by proportional amplifiers in nuclear physics which have been thoroughly reviewed by Danilatos (1990a).

The transfer of nuclear methods and instruments to electron microscopy cannot be readily and generally assumed to work, because microscopy has its own requirements, such as an

extremely fine probe (e.g. 1.5 nm) scanned over a very small raster (e.g. with 1000 lines) at high scanning rates (e.g. 25 frames/s). The limits of imaging are determined by the contrast and resolution which are critically determined by the limiting mechanisms of probe formation, scanning and detection. The practical limits of these parameters are continually improved by new technologies towards their physical limits. For a given method of probe formation, scanning and imaging, it is not clear from the outset how a detector change would affect the other parameters of the instrument. Historically, it required considerable theoretical and practical work and time to establish the GDD of an ESEM as a working equivalent to the proportional amplifier of nuclear physics.

An analogy to the above analysis prevails for a newly proposed detector which is the subject of this paper. It is proposed to replace the static (or d-c) electric field of the GDD with a very fast alternating (or a-c) electromagnetic field. Relatively little work has been previously reported on related methods in nuclear field, which makes it even more difficult to know, or assume, in advance the chances of success of the present proposal. An attempt is made to gather all the necessary material and information upon which the system is based. The background theory for a practical design of a radiofrequency gaseous detection device (RF-GDD) is outlined below so that its feasibility can be assured.

Theory

The idea of replacing the d-c electric field of a GDD with an a-c one may raise some serious questions to the expert in electron microscopy and related fields: (a) Is it possible, in the first place, to oscillate the electrons emanating from the specimen in the conditions of gas pressure, geometry and pixel dwell time required in the microscope? (b) Is the amplitude and frequency of the field required practical to produce? (c) Is the output signal from one pixel distinguishable from the output of the next pixel? (d) Is the alternating field going to disturb the stability of the probe by an amount that could render the probe useless, or have other

adverse effects on the instrument and specimen? (e) Is the design and construction of the detector economical and practical for an ESEM? (f) What are the over all advantages? These questions are dealt with and, by and large, overcome below.

The best approach would be to actually construct an apparatus for testing the idea in the conditions of an electron microscope. However, this is anticipated to be undertaken by the manufacturer, while the present worker provides the principal information requirements.

Some of the earliest papers to deal with gaseous discharges at high field frequencies are traced back to the early decades of this century. Gutton et al. (1923) reported a series of measurements with two wire electrodes 18 mm apart placed inside and normal to the axis of a cylindrical tube with 10 mm diameter. He found that the curves of the breakdown potential versus pressure at fixed frequencies in the range of 50Hz-2 MHz are similar to the shapes of Paschen curves for d-c discharges. The breakdown values of minimum sparking potential steadily increased with frequency, and varied between 375-485 volts in the pressure range of 80-109 Pa. He also placed the electrodes outside the tube at 24 mm apart and found first an increase and then a decrease of the potential versus frequency. Later, (Gutton, 1928) extended the measurements for frequencies close to 100 MHz using a cylindrical tube with 10 cm length and 3 cm diameter with plate electrodes placed outside the tube. The pressures used were below 60 Pa. The curves of the minimum breakdown voltage versus pressure showed a different variation revealing a more complex nature of the discharge than previously found.

Initially, one hopes to apply scaling factors such as the use of the pressure-distance equivalence principle to deduce equivalent conditions for an electron microscope but, unless the complex nature of the underlying discharge mechanisms is understood, the validity of this principle is doubtful. It is unclear how various parameters ought to vary in the presence of radiofrequency fields. Subsequent works by prominent researchers have confirmed these difficulties and a priori assumptions may not be acceptable.

Thomson (1930; 1934; 1936; 1937) undertook and reported extensive investigations of the same subject both theoretically and experimentally over several years. He used plate electrodes at distances between 2.58-20 cm, frequencies between 2-100 MHz and pressures up to 1300 Pa with hydrogen gas. The early theoretical approximations were shown to be inadequate in explaining the full range of observations.

Based on the above works, the shape of curves of the sparking potential versus pressure at various frequencies show the following general characteristics: At low frequencies, the shape is similar to the Paschen curves with d-c potential, but they exhibit higher sparking values. At higher frequencies, a second minimum sparking potential appears and at still higher frequencies only the new minimum appears at progressively lower pressures. The variation is somewhat complex and the reader should consult those works for more information.

Townsend (1938) presented a generalised theory of electrical discharges including d-c and a-c electromagnetic fields and static magnetic fields. However, for the purposes of the present paper, the works reported by Gill (1931) and Gill and Engel (1948; 1949) provide more direct information, from which some selected experimental results are adapted and reproduced below.

The variation of amplitude (peak value) of the electric field versus frequency at breakdown point is plotted in Fig. 1. These measurements were obtained by use of two flat external electrodes, 35.5 mm apart, attached to the flat ends of a sealed cylindrical tube containing pure hydrogen. Three curves have been re-drawn for the fixed pressures indicated. There is a clear and reproducible cut-off frequency at which a sharp change of the field occurs. This characteristic frequency is associated with the transition to a regime where the ionisation is produced entirely in the bulk of the gas. Below the cut-off frequency, the discharge is due to a co-operative action of electrons and ions whereby the ions release electrons from the electrodes and the electrons create further ions in the gas. The magnitude of the field amplitude change is maximum at low pressure, it passes through a minimum value and then it

increases again with pressure. This behaviour is general although not as pronounced with all gases.

Fig. 2 shows a corresponding situation with nitrogen gas, which is often employed in ESEM. The cut-off point is still clearly seen but there is a smoothing effect on the magnitude of field change. This has been attributed to the less synchronised movement of electrons in the gas (as a group) at high frequency, because of the greater velocity distribution of electrons. The latter phenomenon is very pronounced in neon gas where the cut-off points are not well defined. However, for the present purposes, it is important that all gases are governed by the same mechanism at sufficiently high frequencies and pressures, namely, the ionisation is caused by the oscillations of electrons in the bulk of the gas. It is also important that the required field is much lower at high frequency and pressure than at low frequency and pressure. The latter conditions are favoured by ESEM operation and are easier for the construction of the associated hardware.

The use of low frequencies and very low pressures are also included in the present detector as working conditions, although the underlying mechanism of discharge is different. In this regime, the electrons multiply via a production of secondary electrons at the surface of electrodes being struck repeatedly by electrons and ions. When the rate of production exceeds the rate of loss mainly due to diffusion to nearby walls (electrodes, or other), a breakdown occurs. This regime prevails at very low pressure where the mean free path is much larger than the size of the vessel, and not enough gas molecules are around to produce ionisation to sustain the discharge. A plasma situation is not generally reached in the conditions of ESEM operation where the gas can be considered as weakly ionised (see e.g. survey by Danilatos, 1990a). Gill and Engel (1948) have reported the details for the breakdown discharge. They used pressures around 0.1 Pa with inter-electrode distance of 3, 6 and 17.6 cm. They found that above a cut-off frequency a discharge could be established. These conditions may be converted to equivalent ones for an ESEM as follows: At a typical inter-electrode distance of 2 mm, both frequency and pressure must be inversely proportional to the distance. Thus, the

corresponding smallest pressure would be around 2 Pa, which is much lower than ESEM pressures usually being greater than 50 Pa. The possibility of allowing the ESEM to operate also at such low and even lower pressures means that the RF-GDD could act as a universal detector to bridge the gap between SEM and ESEM systems and ultimately unify them.

The understanding of operation of the detection at particularly low pressure is essential. According to Gill and Engel (1948), the observed light emission from the gas was generated from excitation and ionisation of the gas which was not sufficient to maintain the discharge. The discharge was maintained predominantly by the secondary electrons produced at the electrode by those charged particles which acquire the necessary energy. For a detailed mathematical analysis, the original work should be consulted. However, for this approach to be used as detector in a microscope, we have to provide additional controls: We must allow the electron multiplication to take place but we must also simultaneously drain the produced current away so that the discharge is extinguished when there is no initial supply of electrons in the a-c field. The drainage of charge is controlled by appropriate collection electrodes. This can be achieved by proper configuration of the a-c electrodes together with a set of d-c electrodes, or generally by superimposing a d-c with the a-c field so that the current is collected while it is amplified, always prior to the onset of breakdown. The use of the electrode surfaces as electron multipliers would be analogous to continuous channel or dynode electron multipliers where a d-c potential drives an initial electron to repeatedly strike the surfaces and produce an avalanche multiplication. In the present system, the gas plays a gradually increasing role in the multiplication process as we increase the pressure, until eventually the gas becomes the sole controlling mechanism for the detector.

Now, we analyse closer the regime usually employed in an ESEM. For reference, let us consider the typical case of D=2 mm and p=1000 Pa. An electron released from the specimen surface in the gas will undergo several collisions before it reaches an anode in the presence of an electric field E. A steady state velocity, the drift velocity v_d, is proportional to the applied field

$$v_d = KE \qquad (1)$$

where K is the electron mobility. When the applied field E is alternating with amplitude E_0 and frequency f as

$$E = E_0 \sin 2\pi ft \qquad (2)$$

the velocity remains in phase with the force (i.e. at sufficiently high pressure) so that the equation of motion is

$$\frac{dx}{dt} = KE_0 \sin 2\pi ft \qquad (3)$$

A simple integration yields the peak amplitude of displacement to be

$$x_0 = \frac{KE_0}{2\pi f} \qquad (4)$$

so that the total displacement, being twice the peak value, cannot exceed the inter-electrode distance D. This determines the cut-off frequency f_c at which we get

$$D = \frac{2KE_0}{2\pi f_c} = \frac{v_0}{\pi f_c} \qquad (5)$$

From the latter equation, we can find the drift velocity if we know the cut-off frequency, or we can find the cut-off frequency if we know the drift velocity. The drift velocity can also be derived from knowledge of the electron mobility, as given by Healy and Reed (1941):

$$v_d = \frac{2eL'}{3um}\frac{E}{p} \qquad (6)$$

where L' is the mean free path at unit pressure, u the thermal velocity of the electron and e and m the charge and mass of the electron. Combining Eqs. (5) and (6) we can derive the cut-off frequency by

$$f_c = \frac{2eL'}{3\pi Dum}\frac{E_0}{p} \qquad (7)$$

From Fig. 2, we find that the frequency just after the cut-off point is 6.5 MHz and the field 5.8 kV/m for the case of 26.7 Pa. The pressure distance product for this case is pD=0.95 Pa·m. For an ESEM distance D=2 mm, in order to maintain constant pD, we find that the corresponding pressure is 474 Pa (and the equivalence factor is 35.5/2=17.75). The field amplitude must be increased by the same proportion which is achieved by keeping the same potential of about 206 V. The electron acquires the same energy over the shorter total distance it travels, or over the shorter mean free path, and produces the same average number of collisions. The drift velocity remains the same in the two corresponding cases because this quantity is assumed to depend only on the E/p ratio, which remains constant in the two cases. Therefore, the transit time should be inversely proportional to the distance. All these parameters can be deduced from published data. Measurements for a wider range of pressures are first adapted and reproduced in Figs. 3 and 4 taken for the case D=35.5 mm from Gill and Engel (1949). They are then used to deduce the corresponding curves for the cut-off frequency and sparking field with nitrogen for ESEM in Fig. 5.

For easy reference and discussion, some calculated values are also given in Table 1 in which we include pressure, frequency, field amplitude, potential amplitude, drift velocity and transit time. As transit time we have taken half the period T of the oscillation which is given for the cut-off condition.

The transit time becomes shortest in vacuum, actually when the electron ceases to collide with gas molecules below some very low pressure. In this case, we can find the transit time *t* from the simple equation

$$t = \sqrt{\frac{2m}{eV}} D \qquad (8)$$

As an example, for V_c=368 V, we find *t*=0.35 ns in vacuum as compared to 7.9 ns for nitrogen at 3000 Pa according to Table 1. This indicates the significant effect of the gas in slowing down the electrons. However, the transit times still remain extremely short, much shorter than the shortest typical pixel time used in ESEM. For example, an image recorded with 1000 lines over 1 s corresponds to 1 MHz. TV scanning rates can be conveniently achieved at around 10 MHz. This implies that we can apply 5-20 oscillations during the pixel dwell time to reach the frequencies required for an electron to oscillate inside the bulk of the gas. This is an excellent finding which shows that the principle proposed herewith is compatible with the time scales used in ESEM. The slowing down of electrons by the gas is progressively diminished as we lower the pressure. Equations (5) and (6) lose their validity below some minimum pressure, the level of which strongly depends on the nature of gas. For nitrogen, these equations are safe to use above, say 1000 Pa. For low pressures, the mathematical treatment of this subject becomes quite complex, but the basics of the present detector remain in force.

Next we should consider possible effects on the imaging process. The critical values of frequency and potential quoted above are not to be used in ESEM because a breakdown would saturate the image. The actual frequency must be greater and the field less than the corresponding critical values. In fact, we can reduce the potential to any convenient value that would still allow sufficient amplification without any adverse discharge. Let's assume that we reduce it to a point where only one electron is freed for each transit and there are ten transits during the pixel dwell time. In this case, the multiplication factor would be 2^{10}=1024. If we assume that two electrons are released for each electron, for each transit, then the amplification

factor becomes 3^{10}=59049. Such factors are far superior than the best situation in a d-c discharge as practised up to the present. However, the fundamental consideration still remains whether such high gains are actually achievable before a breakdown takes place in the a-c field, which would be the case if the mechanisms of breakdown were the same as in the d-c field.

Previously, a thorough survey was undertaken by Danilatos (1990a) into the physical limitations of the d-c discharge used as an amplifier. It has been shown that the maximum practical gain is controlled primarily by the secondary, or γ-processes which are operating singly, or simultaneously. These processes are responsible for the injection of new electrons from the cathode, over and above the electrons produced directly in the gas by the transiting electrons. It is the γ-processes which cause the breakdown and limit the gain, and if we could somehow eliminate them, or reduce them, then we would increase the gain to very high values. Eventually, even in the absence of γ-processes, a breakdown will eventually occur due to the very high concentration of electron density at the head of the avalanche, but the point remains that an improvement should be expected if we reduce the γ-processes. In this connection, we re-visit the actual mechanisms for these processes which are: (a) Positive ions strike the cathode and release electrons. (b) The photons in the avalanche eject photoelectrons from the cathode. (c) Metastables release electrons from the cathode. The importance of these mechanisms is in the same order.

It is suggested that ions produced under an a-c field should not liberate additional ions from the cathode because they initially remain in the bulk of the gas. We must, of course, extract them as soon as possible, but this extraction can now be controlled with an additional small d-c bias. The intensity of this additional bias can be low enough not to impart sufficient energy to the ions to enable them to eject electrons from the cathode. This is a significant advantage which is expected to improve the performance of the detector. Based on the information published in the literature, it is expected that the gain should be very high. In the unlikely worse case, the gain cannot be worse than the standard GDD operating under a d-c field, and the RF-GDD still remains possible and compatible with ESEM.

The presence of ions has an important effect on image quality via their own transit times, concentration and distribution. The effects of ions on imaging have been discussed in detail elsewhere (Danilatos, 1990a; 1990c), and it can be shown that correct electrode configuration can greatly improve the performance of the detector. Similar effects are expected to appear in the new situation with a probably larger population of ions, the drift energy of which can be controlled by the ancillary d-c potential. The general principle is that any ions which cannot respond and follow the fast variation of the electron signal contribute to the background component of noise. The net result of increasing the gain of both useful and background signals is an improvement of the detector.

The time response of the system is improved, and some problems that the ions may cause can be overcome by collecting the photons produced in the generated avalanche. The light emitted is primarily produced during the initial transit of the electron, and its detection constitutes a most appropriate manner of operation (for details, see literature survey in Danilatos, 1990a). Light is produced both by (a) molecules excited by the transiting electrons and (b) by recombination of ions. Generally, the former mechanism is predominant, very fast and practically synchronous with the amplification of the electron avalanche, while the latter contributes to a weak background noise level. Light has already been used to produce secondary electron imaging at true TV scanning rates with the GDD by Danilatos (1992). Further, use of light instead of charge has some additional unique advantages, especially if we use spectroscopic means for differentiating its various components corresponding to different production mechanisms and hence to unique contrasts and resolutions. The intense production of light in electrodeless discharges has been reported previously, especially for use by spectroscopists (Nisewanger et al., 1946). It has further been used in nuclear technology for evaluation of a digital optical ionising radiation particle track detector (Hunter, 1987) and for digital characterisation of recoil charged particle tracks for neutron measurements (Turner et al. 1989).

Another remaining crucial question relates to the stability of the scanned probe of an instrument in the presence of an a-c field. In modern microscopes, probes with 1.5 nm diameter are common-place, which means that any interference that could produce an effect greater than the probe size is unacceptable. Indeed, the presence of a radiofrequency field of sufficient amplitude can, in principle, adversely affect the beam. This has been the greatest unknown parameter for some time during the present development. Remedies for this problem now are any, or a combination, of the following means: (a) The applied field is axially symmetric, where it can be shown that the beam is not affected to any appreciable extent. (b) The field is applied at sufficiently long distance from the probe so as to minimise any effects. (c) The beam is shielded by an additional electrode around the beam.

The RF-GDD is not limited to using an a-c electric field, because the application of an alternating electromagnetic field as that produced by a coil through which an alternating current passes, is also possible, and produces an equivalent result as shown by Nisewanger et al. (1946). In view of the radiofrequency range required, a few coil turns can be sufficient to achieve our objective. This implies that such a coil would be possible to incorporate on a number of instruments and the engineering considerations for its integration are left to the manufacturer.

Another variation and improvement of the RF-GDD is to superimpose a static magnetic field parallel, or normal to the a-c field. With such an addition, Townsend (1948) has shown an increased rate of ionisation, and this can be used to advantage in the present detector. It again reduces to an engineering application at the manufacturing level in order to incorporate this advantage into a particular application.

Design, construction and operation of the RF-GDD

Based on the previous analysis, we outline the general approach for the construction and design of a RF-GDD. Referring to Fig. 6, a charged particle beam focussed and scanned by means of electron optics passes through an aperture and a gas layer before it impinges on a specimen. The distance travelled by the beam in the gas is such that sufficient number of particles remain in the original focussed spot, while the remainder of the beam is scattered by gaseous collisions clearly away from the focussed spot. An annular plate electrode (rf) is placed some distance above the specimen and is biased with an alternating electric field of variable frequency and amplitude. A second concentric electrode (collector) shown as a wire ring is inserted for the purpose of superimposing a d-c electric field in the volume acted upon by the a-c field and for collecting the amplified signal. A further concentric electrode (collector/shield) is placed at the innermost position around the beam. The latter electrode may be grounded or biased with a d-c potential and it can act either as shield for the beam, or as signal collector, or both. The electrodes are insulated from each other with appropriate insulating material. Light pipes (PMT) may also be inserted to collect the light generated in the gaseous volume. Any or all of the electrodes (including the rf electrode) are connected to the input of electronics amplifiers and the light pipes are connected to the input of photomultipliers, or other photo-detecting devices.

The operation of the above system takes place as follows: The focussed spot of the beam interacting with the specimen releases various signals such as secondary electrons, backscattered electrons, x-rays and other photons. The spot is usually scanned in a raster form over distinguishable pixels having the size of the incident spot. Usually, more than a million pixels are scanned during one second, but this varies according to the operator's needs and instrument specifications. During the very short dwell time over a pixel, the ionising radiations generated by each pixel element of the specimen enter the environmental gas and are acted upon by various fields. The radiofrequency field oscillates the electrons and multiplies them while the superimposed static bias collects the produced charge. The potentials applied are such that a breakdown is avoided and the process is repeated for every pixel. The amount of charge collected for every pixel is proportional to the source intensity, so that as the probe

scans the specimen surface, the collected signal (current, or light) corresponds to the variable properties of the specimen from pixel to pixel. The output from the system is recorded by appropriate means, usually in the form of an image (e.g. on a photograph, or screen monitor) corresponding to the very small raster scanned and representing a high magnification and high resolution image of the specimen under examination.

Discussion

A new detection device has been proposed suitable for instruments employing charged, focussed and scanned beams, such as SEM, ESEM, STEM and ion beam technologies. The novel idea is to use an rf-field instead of a dc-field to generate a controlled discharge in a gaseous environment that is consistent with the operational requirements of such instruments. The same idea can also be used for a new proportional particle detector in particle physics involving ionising radiations.

The generation of an rf-field and other ancillary equipment is well known and standard technology. Reference to the cited literature would facilitate these technological matters but modern approaches may well supersede the older approaches. The rf-generation, modulation-demodulation and related techniques are well developed and fall outside the scope of this paper. The rf-field at breakdown condition is extensively used for generation of ion sources used in various technologies. Ion guns can be made in this way, and for detailed information the reader may refer elsewhere (Wilson and Brewer, 1973; Stuart; 1983; Franks, 1978; Eubank et al., 1954; Swann and Swingle, 1952; Williams, 1966).

The electrical energy requirements of the established GDD are minimal on account of the very low currents, in absolute terms, used in an ESEM. The corresponding energy requirements of a RF-GDD would only increase in proportion to an anticipated gain improvement but the total energy consumption should remain minimal in an electron microscope. The wavelengths λ of

the rf field derived from $\lambda f=c$ (velocity of light) for the frequencies considered herewith are much greater than the dimensions of the main instrument. In relation to these conditions, its construction entails no serious complications. The device can be readily integrated with other components of electron/ion microscopes and instruments, such as with pressure limiting apertures and electron optics. Over all, the new detector aims at producing some distinct advantages:

The gain is expected to be significantly higher than the gain of the d-c GDD. This will generally improve contrast and resolution on account of improved signal-to-noise ratio. The noise propagation in detection systems of SEM and ESEM has been analysed in detail elsewhere and the reader may find it helpful to refer to that work (Danilatos, 1993). Considerations of noise propagation and separation of useful signal from background noise point to a better image contrast. This, in turn, allows the use of beams with less energy and less current which reduce specimen irradiation effects and damage, facts which indirectly improve resolution (on account of smaller beam-specimen interaction volume and specimen detail durability during observation). Accordingly, faster scan rates can be used with better signal-to-noise ratio. The faster rates, in turn, mean the possibility of observing new phenomena and applications not previously accessible.

The RF-GDD allows the detection and amplification of signals in a gaseous environment of relatively low pressure, much lower than the minimum required for the d-c GDD. According to the evidence produced, the detector would also operate at high pressures with even greater ease. Therefore, it is envisaged that, eventually, the new detector will cover the complete pressure range from vacuum to atmospheric pressure.

A further advantage is the elimination of polarisation effects that can manifest themselves on insulators in the presence of strong d-c electric fields . Because the field is alternating at high speed, and because the amplitude is generally smaller, the polarisation cancels out and vanishes (Thomson, 1937).

Finally, the new detector expands the possibilities and alternative technological developments in related industries, which can lead to better and improved instruments for the scientist to choose.

Conclusion

An attempt has been made to show that the RF-GDD is both feasible and useful. The main considerations raised at the outset have bee addressed in this paper. Thus, it is possible to oscillate the electron signal produced from the specimen in the conditions of an ESEM. There is enough time to distinguish the amplified current from pixel to pixel. The a-c field is unlikely to perturb the incident probe by any appreciable amount. The required frequency range and amplitude of oscillation are feasible and compatible with the conditions of a microscope. The hardware requirements are minimal and within the capabilities of established technologies. The new detector is expected to produce an improved performance over the present practice in ESEM.

Journal Articles

Danilatos GD (1986) Cathodoluminescence and gaseous scintillation in the environmental SEM. Scanning, 8:279-284.

Danilatos GD (1988) Foundations of environmental scanning electron microscopy. Adv. Electronics Electron Phys. 71:109-250.

Danilatos GD (1990a) Theory of the gaseous detector device in the environmental scanning electron microscope. Adv. Electronics Electron Phys. 78:1-102.

Danilatos GD (1990b) Mechanisms of detection and imaging in the ESEM. J. Microsc. 160:9-19.

Danilatos GD (1990c) Equations of charge distribution in the environmental scanning electron microscope (ESEM). Scanning Microsc. 4:799-823.

Danilatos GD (1992) Secondary electron imaging by scintillating gaseous detection device. Proc. 50th Annual Meeting EMSA. San Francisco Press, San Francisco pp 1302-1303.

Danilatos GD (1993) Environmental scanning electron microscope: Some critical issues. Scanning Microsc. Intern. Supplement 7, 1993:57-80.

Eubank HP, Peck RA and Truell R (1954) Operating characteristics of a high rf ion source. Rev. Sci. Instr. 25:989-995.

Franks J (1978) Ion beam technology to electron microscopy. Adv. Electronics Electron Phys. 47:1-50.

Gill EWB (1931) The sparking potential of air for high frequency discharges. Phil. Mag. 12:719-726.

Gill EWB and Engel A (1948) Starting potentials of high-frequency gas discharges at low pressure. Proc. Roy. Soc. A 192:446-463.

Gill EWB and Engel A (1949) Starting potentials of electrodeless discharges. Proc. Roy. Soc. A 197:107-124.

Gutton C, Mitra SK and Ylostalö V (1923) Sur la décharge à haute fréquence dans les gas rar éfiés. Comptes Rendus 176:1871-1874.

Gutton C and H (1928) Sur la décharge électrique en haute fréquence. Comptes rendu 186:303-305.

Hunter SR (1987) Evaluation of a digital optical ionising radiation particle track detector. Nucl. Instr. Meth. Phys. Res. A260:469-477.

Nisewanger CR, Holmes JR and Weissler GL (1946) Electrodeless discharges at high frequencies and low pressures. J. Opt. Soc. Amer. 36:581-587.

Swann CP and Swingle JF (1952) Radiofrequency ion source. Rev. Sci. Instr. 23:636-638.

Thomson J (1930) On the mechanism of the electrodeless discharge. Phil. Mag. 10: 280-291.

Thomson J (1934) The high frequency glow discharge. Phil. Mag. 18: 696-719.

Thomson J (1936) A new polarisation effect in discharge tubes. Phil. Mag. 21:1057-1066.

Thomson J (1937) Sparking potentials at ultra-high frequencies. Phil. Mag. 23:1-24.

Townsend JS (1938) Generalisation of the theory of electrical discharges. Phil. Mag. 26:290-311.

Turner JE, Hunter SR, Hamm RN and Wright HA (1989) Digital characterisation of recoil charged particle tracks for neutron measurements. Nucl. Instr. Meth. Phys. Res. B40/41:1219-1223.

Williams JF (1966) Extraction of positive ions from electrodeless discharge. Rev. Sci. Instr. 37:1205-1210.

Books

Healey RH and Reed JW (1941) The behaviour of slow electrons in gases. Sydney: Amalgamated Wireless (Australasia) Ltd.

Stuart RV (1983) Vacuum Technology, Thin Films, and Sputtering. Orlando: Academic Press, Inc.

Wilson RG and Brewer GR (1973) Ion Beams with Applications to Ion Implantation. New York: John Wiley & Sons.

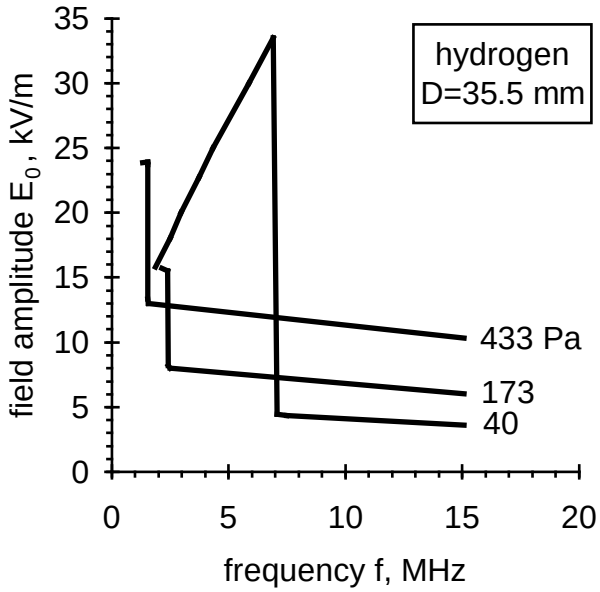

Fig. 1 Variation of peak values of sparking field versus frequency in hydrogen at fixed pressures indicated with each curve.

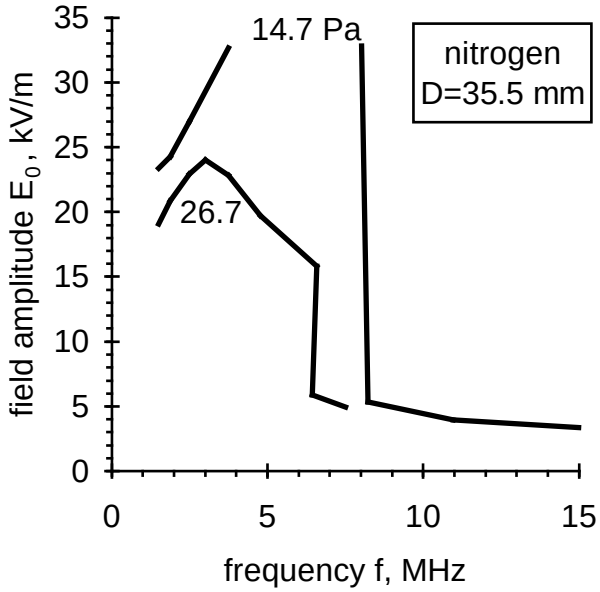

Fig. 2 Variation of peak values of sparking field versus frequency in nitrogen at fixed pressures indicated with each curve.

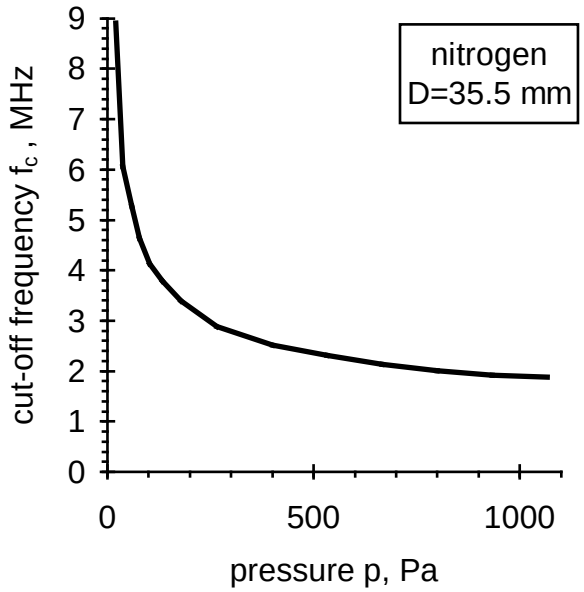

Fig. 3 Variation of the cut-off frequency versus pressure in nitrogen.

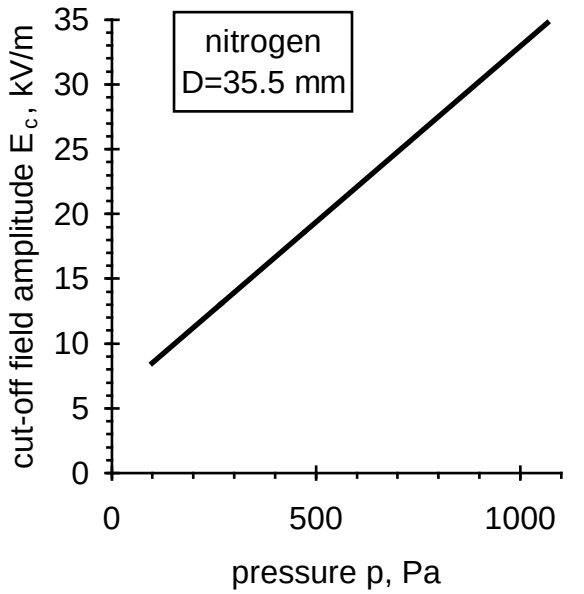

Fig. 4 Variation of the breakdown field amplitude at cut-off frequency versus pressure in nitrogen.

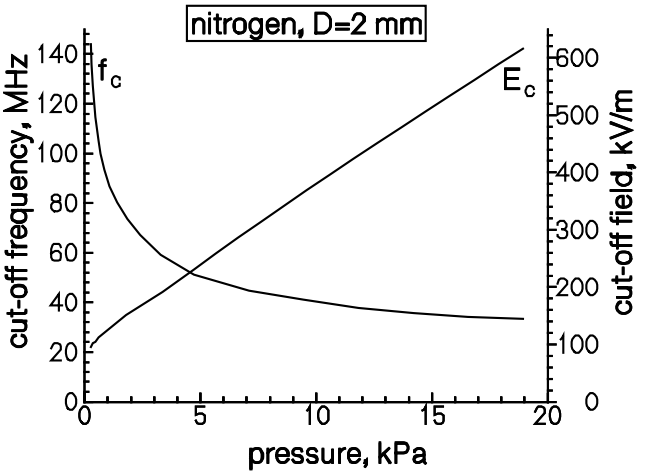

Fig. 5 Variation of frequency and field amplitude at cut-off condition in ESEM.

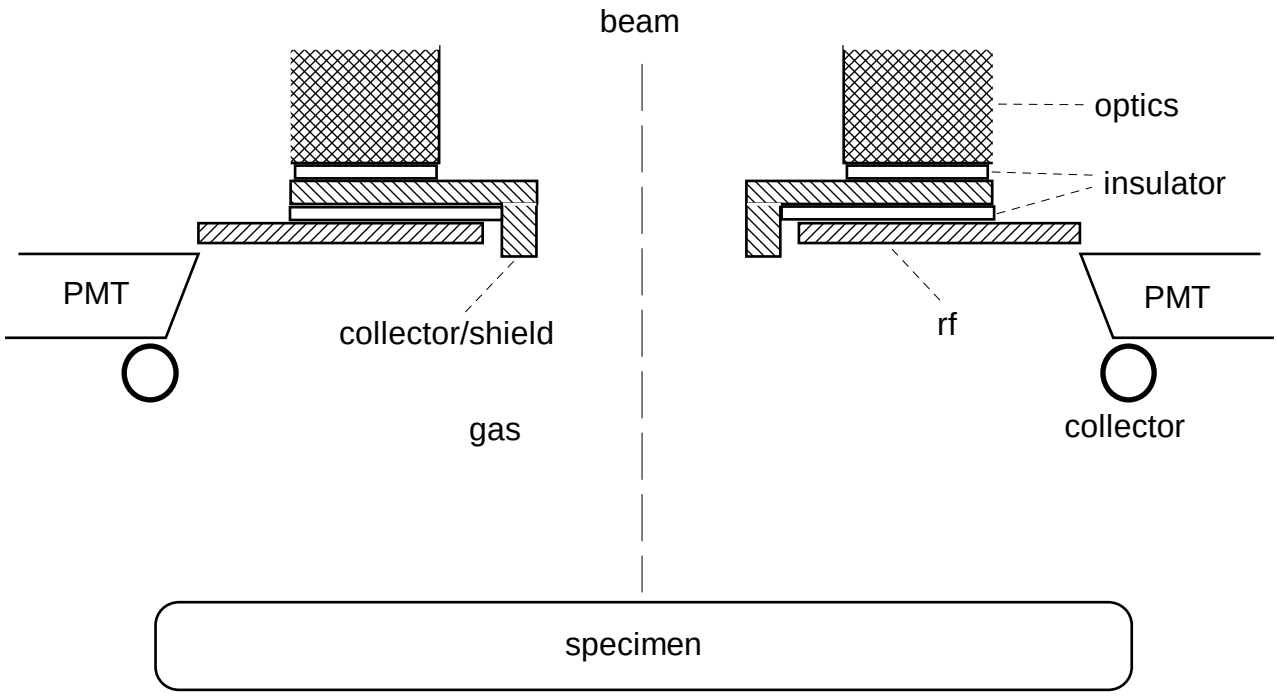

Fig. 6 Schematic of a general RF-GDD in an ESEM.

ESEM parameters for D=2 mm				
p, Pa	f_c, MHz	E_c, kV/m	V_c, Volts	$T/2$, ns
300	137.0	98.0	196.0	3.65
400	122.4	102.9	205.8	4.08
500	112.3	105.8	211.6	4.45
600	104.4	112.3	224.6	4.79
700	99.4	115.6	231.2	5.03
800	97.6	118.9	237.8	5.12
900	95.6	122.2	244.4	5.23
1000	93.7	125.5	251.0	5.33
1500	84.0	142.0	284.0	5.95
2000	74.5	157.2	314.4	6.71
2500	66.3	171.0	342.2	7.54
3000	63.0	184.0	368.0	7.94

Table 1. Pressure p, frequency f_c, field amplitude E_c, potential amplitude V_c, and transit time $T/2$ for inter-electrode distance D with nitrogen at cut-off condition in ESEM.